Cell Reports Medicine, Volume *5*

Supplemental information

Gene therapy for diffuse pleural mesotheliomas in preclinical models by concurrent expression of *NF2* and *SuperHippo*

Rui Zhu (朱锐), Xincheng Liu (柳鑫成), Xu Zhang (张栩), Zhenxing Zhong (钟振兴), Sixian Qi (祁思娴), Ruxin Jin (靳茹炘), Yuan Gu (顾远), Yu Wang (王瑜), Chen Ling (凌晨), Kang Chen (陈康), Dan Ye (叶丹), and Fa-Xing Yu (余发星)

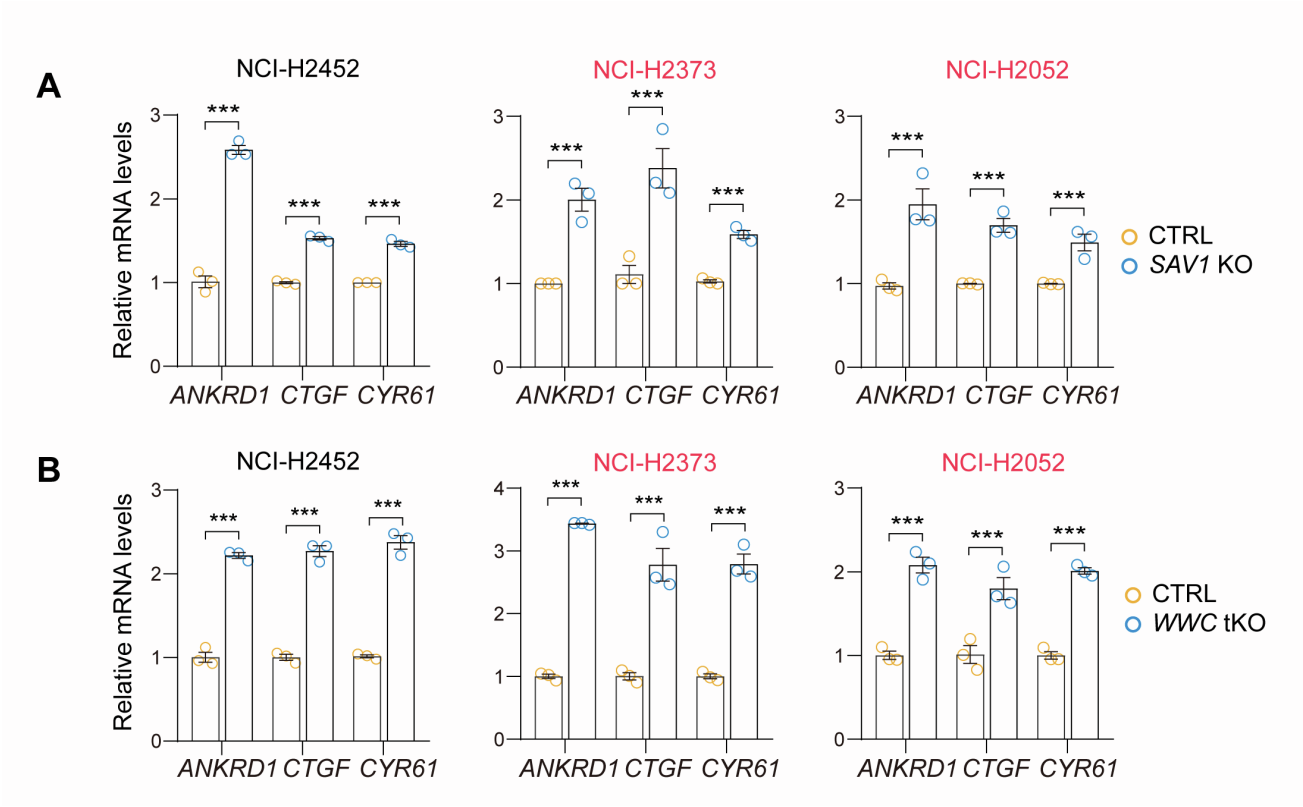

Figure S1. Deletion of *SAV1* or *WWC1-3* induces expression of YAP/TAZ target genes. Related to Figure 1.

(A) Upregulated mRNA levels of YAP/TAZ target genes *ANKRD1*, *CTGF*, and *CYR61* in *SAV1* KO DPM cells.

(B) Upregulated mRNA levels of YAP/TAZ target genes in *WWC1-3* KO DPM cells.

Data are presented as mean ± SEM from three independent experiments. Statistical significance: *, $p < 0.05$, **, $p < 0.01$, ***, $p < 0.001$. Student's *t*-test.

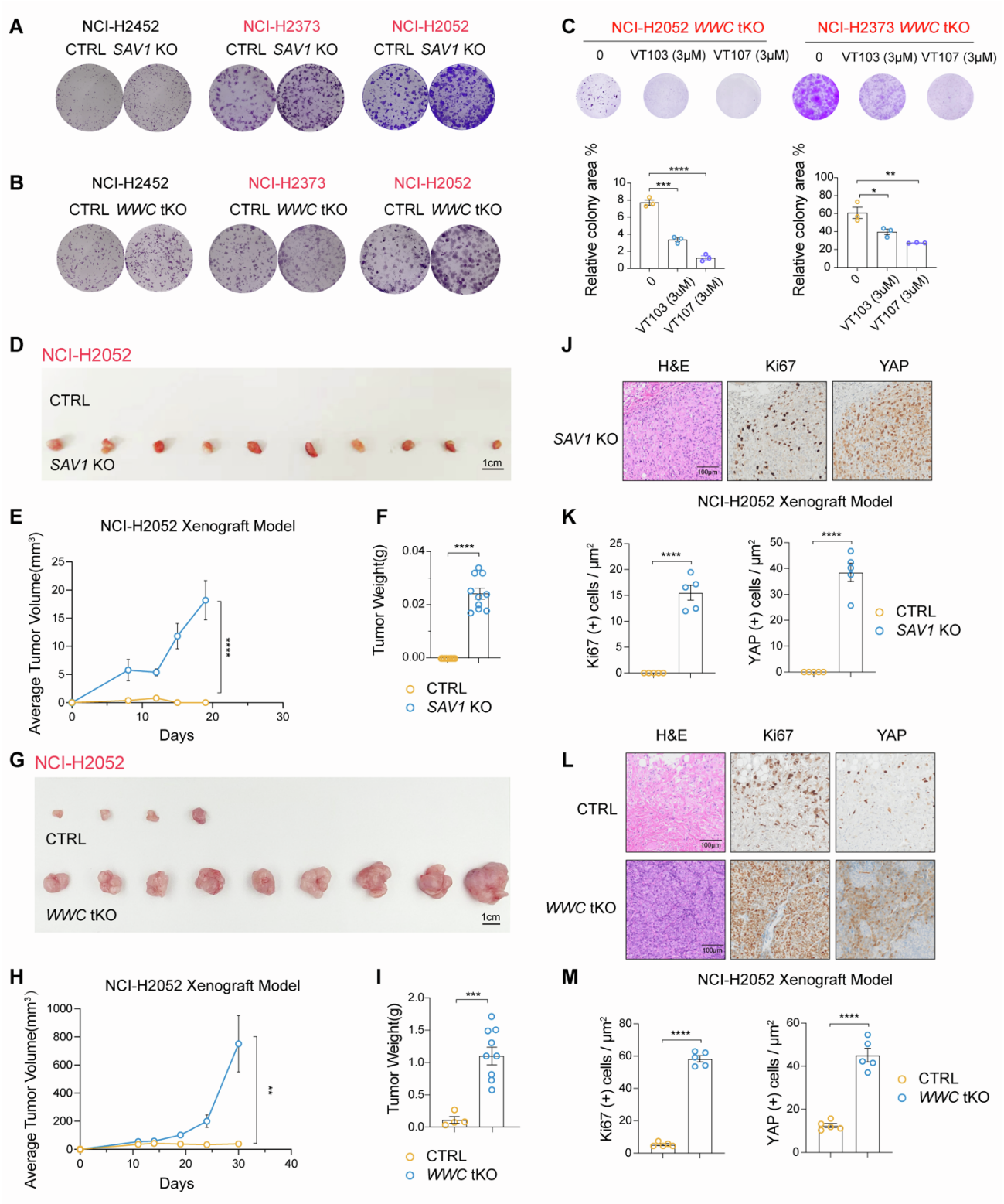

Figure S2. Downregulation of *SAV1* or *WWC1-3* expression promotes the tumor-forming capacity of DPM cells. Related to Figure 2.

(A and B) Crystal violet staining of colonies in *SAV1* or *WWC1-3 KO* mesothelioma cell lines.

(C) VT103 and VT107 block colony formation of *WWC1-3* KO NCI-H2052 and NCI-H2373 cells.

(D) Gross tumor images of xenografts derived from *SAV1* KO NCI-H2052 cells implanted in nude mice. Scale bar, 1 cm.

(E and F) Growth curve and tumor weight analysis of control and *SAV1* KO NCI-H2052 tumor xenografts. Five mice and 10 tumors for each group were analyzed.
(G) Gross tumor images of xenografts derived from *WWC1-3* KO NCI-H2052 cells implanted in nude mice. Scale bar, 1 cm.
(H and I) Growth curve and tumor weight analysis of control and *WWC1-3* KO NCI-H2052 tumor xenografts. Five mice and 9 tumors for each group were analyzed.
(J and K) Histological assessment of *SAV1* KO NCI-H2052 tumor xenografts. H&E and IHC (Ki67 and YAP) staining and quantifications. Scale bar, 100 μm.
(L and M) Histological assessment of control and *WWC1-3* KO NCI-H2052 tumor xenografts. H&E and IHC (Ki67 and YAP) staining and quantifications. Scale bar, 100 μm.
Data are presented as mean ± SEM. Statistical significance: *, $p < 0.05$, **, $p < 0.01$, ***, $p < 0.001$. The Two-way ANOVA test was used for tumor growth curves (D, I), and the Student's *t*-test was used for other data.

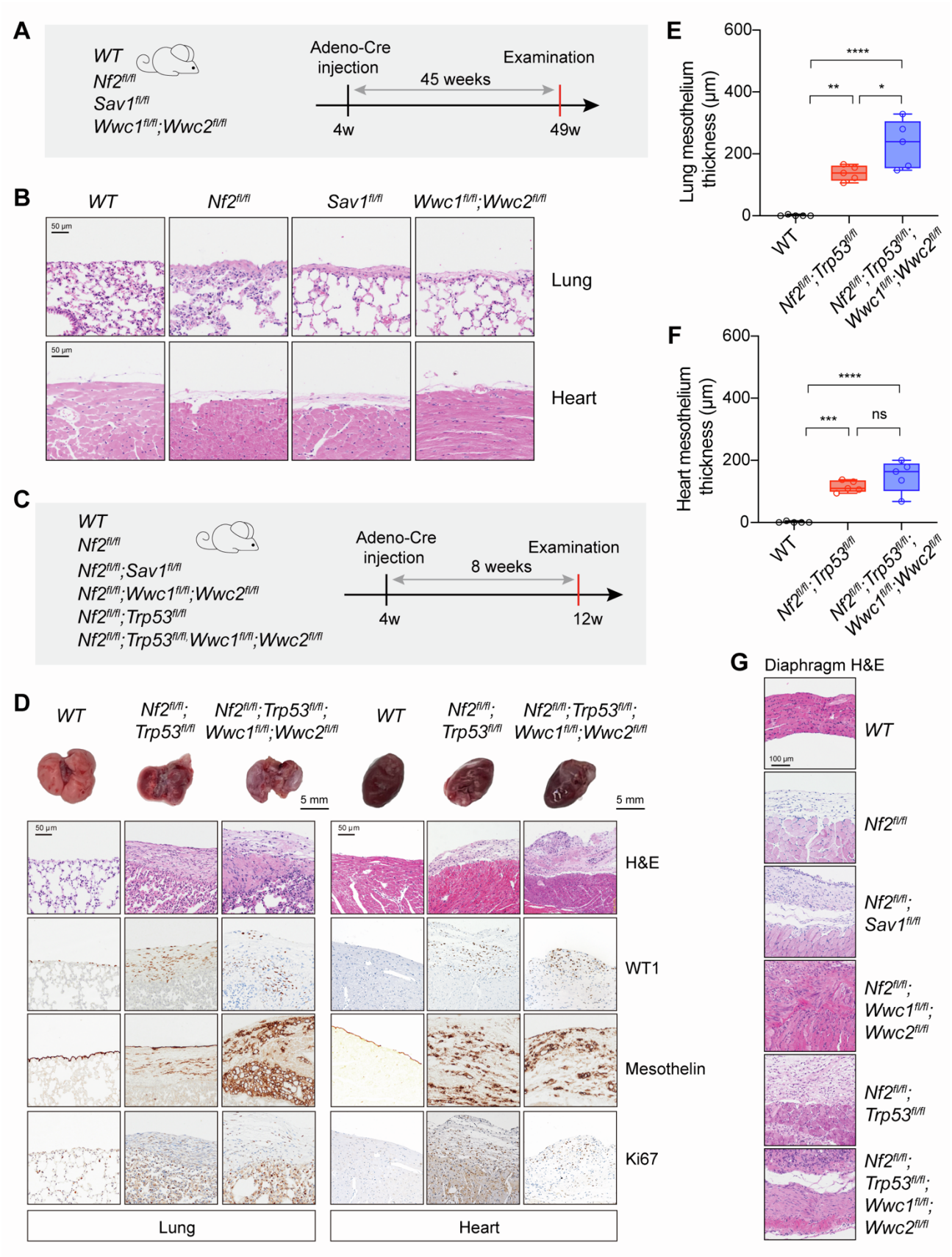

Figure S3. Accelerated mesothelioma development upon *Sav1* or *Wwc1/2* deletion in the mesothelium of pleural cavities. Related to Figure 3.

(A) Schematic diagram indicating experimental procedure. Mice (n = 3-5 per group) at 4-week-old were injected with Adeno-Cre to delete corresponding genes, lungs and hearts were collected after 45 weeks for histological analysis.
(B) H&E staining of lungs and hearts from mice with different genotypes. Scale bar, 50 μm.
(C) Schematic diagram indicating experimental procedure. Mice (n = 5 per group) at 4-week-old were injected with Adeno-Cre to delete corresponding genes, lungs and hearts were collected after 8 weeks for histological analysis.
(D) H&E and IHC staining of lungs and hearts from mice with different genotypes. The expression of WT1, Mesothelin, and Ki67 were determined by IHC. Scale bars, 5 mm for gross organ images, and 50 μm for H&E or IHC images.
(E and F) Quantification of the average thickness of lung and heart mesothelium in mice with different genotypes. Mesothelium thickness is primarily defined by Mesothelin staining signals.
(G) H&E of diaphragms from mice with different genotypes. Tissues were collected 8 weeks after Cre induction. Scale bar, 100 μm.
Data are presented as mean ± SEM. Statistical significance: *, $p < 0.05$, **, $p < 0.01$, ***, $p < 0.001$. The Student's *t*-test was used for statistical analysis.

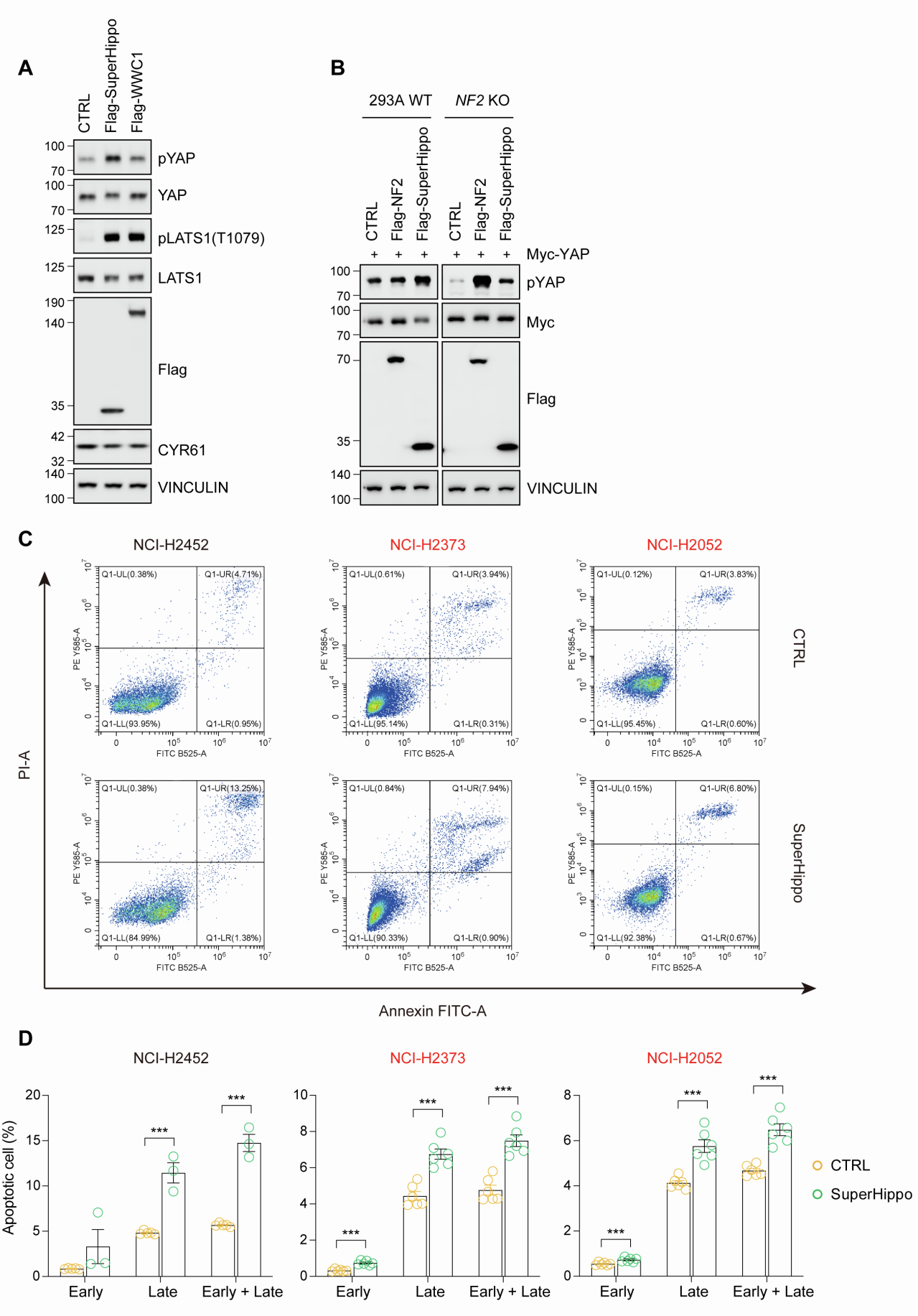
A
CTRL
Flag-SuperHippo
Flag-WWC1
pYAP
YAP
pLATS1(T1079)
LATS1
Flag
CYR61
VINCULIN
B
293A WT
NF2 KO
CTRL
Flag-NF2
Flag-SuperHippo
Myc-YAP
pYAP
Myc
Flag
VINCULIN
C
NCI-H2452
NCI-H2373
NCI-H2052
CTRL
SuperHippo
PI-A
Annexin FITC-A
PE Y585-A
FITC B525-A
Q1-UL(0.38%)
Q1-UR(4.71%)
Q1-LL(93.95%)
Q1-LR(0.95%)
Q1-UL(0.61%)
Q1-UR(3.94%)
Q1-LL(95.14%)
Q1-LR(0.31%)
Q1-UL(0.12%)
Q1-UR(3.83%)
Q1-LL(95.45%)
Q1-LR(0.60%)
Q1-UL(0.38%)
Q1-UR(13.25%)
Q1-LL(84.99%)
Q1-LR(1.38%)
Q1-UL(0.84%)
Q1-UR(7.94%)
Q1-LL(90.33%)
Q1-LR(0.90%)
Q1-UL(0.15%)
Q1-UR(6.80%)
Q1-LL(92.38%)
Q1-LR(0.67%)
D
NCI-H2452
NCI-H2373
NCI-H2052
Apoptotic cell (%)
Early
Late
Early + Late
***
CTRL
SuperHippo

Figure S4. Activation of Hippo signaling pathway by SuperHippo expression in an NF2-independent manner. Related to Figure 4.

(A) Expression of SuperHippo effectively activated the Hippo signaling pathway in WT HEK293A cells.

(B) Expression of SuperHippo induced phosphorylation of LATS1/2 and YAP and decreased CYR61 expression in WT or *NF2* KO HEK293A cells.

(C) The Annexin V-FITC/PI staining assay was performed to detect apoptosis induced by SuperHippo expression in mesothelioma cell lines. Representative flow cytometry plots were shown.

(D) Quantification of apoptotic cell percentages in mesothelioma cell lines between control and SuperHippo groups. Data are presented as mean ± SEM from three or six independent experiments. Statistical significance: *, $p < 0.05$, **, $p < 0.01$, ***, $p < 0.001$. Student's *t*-test was used.

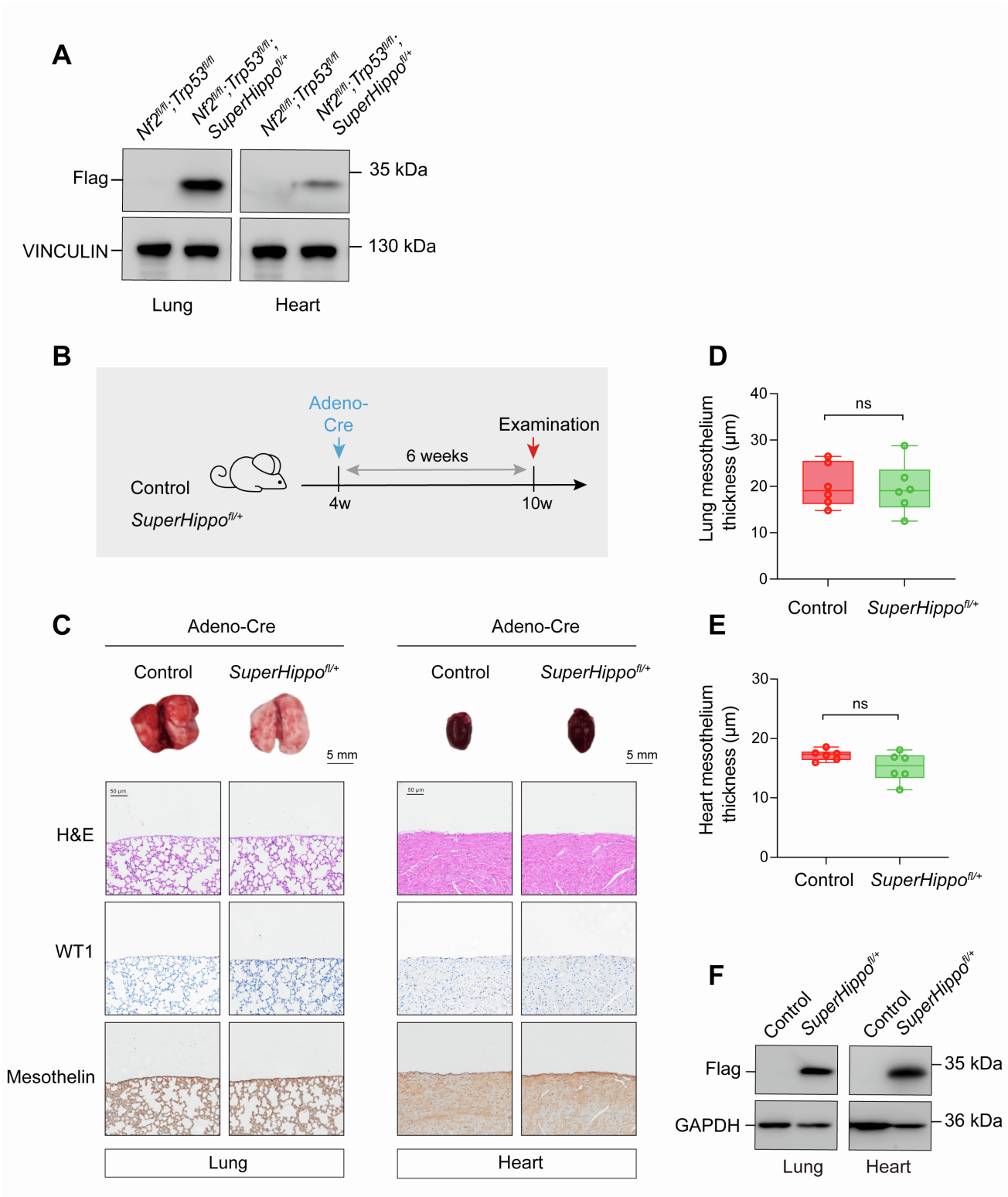

Figure S5. Expression of SuperHippo in mouse mesothelium has no evident phenotype. Related to Figure 5.

(A) Immunoblotting of SuperHippo expression (Flag tag) in lung and heart of *Nf2*$^{fl/fl}$;*Trp53*$^{fl/fl}$ and *Nf2*$^{fl/fl}$;*Trp53*$^{fl/fl}$;*Superhippo*$^{fl/+}$ mice.

(B) Schematic diagram indicating experimental procedure. Mice (n = 3 per group) at 4-week-old were injected with Adeno-Cre to induce SuperHippo expression in the pleural mesothelium. After 4 weeks, lungs and hearts were collected for histological analysis.

(C) Gross image and histological analysis of lungs and hearts. H&E and IHC staining for WT1 and Mesothelin was performed. Scale bar, 5 mm for gross images, and 50 μm for H&E or IHC images.
(D and E) Quantification of the average thickness of lung and heart mesothelium. Mesothelium thickness is primarily defined by Mesothelin staining signals.
(F) Immunoblotting of SuperHippo expression in lung and heart of mice.

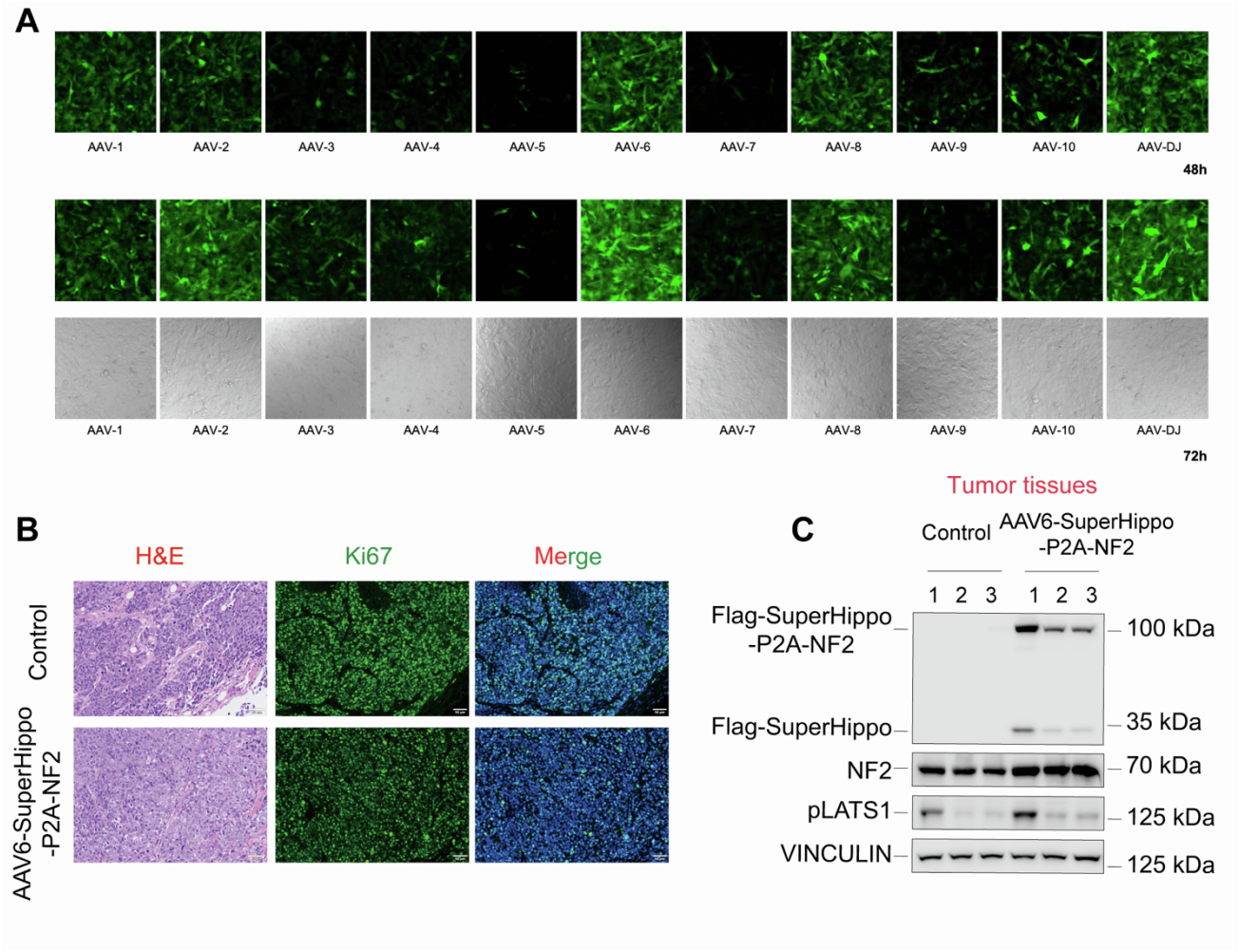

Figure S6. AAV6-mediated expression of *SuperHippo-P2A-NF2* in DPM tumors. Related to Figure 6.

(A) Assessment of transduction efficacy of various AAV serotypes in NCI-H2052 cells. GFP signal indicates viral transduction and ectopic protein expression. DIC images indicate cell density.

(B) H&E and Ki67 immunostaining of xenograft tumors treated with AAV6-control or AAV6-*SuperHippo-P2A-NF2*. Scale bars, 50 μm.

(C) Expression and cleavage of *SuperHippo-P2A-NF2* in *WWC tKO* NCI-H2052 mesothelioma cells treated with AAV6-*SuperHippo-P2A-NF2*.

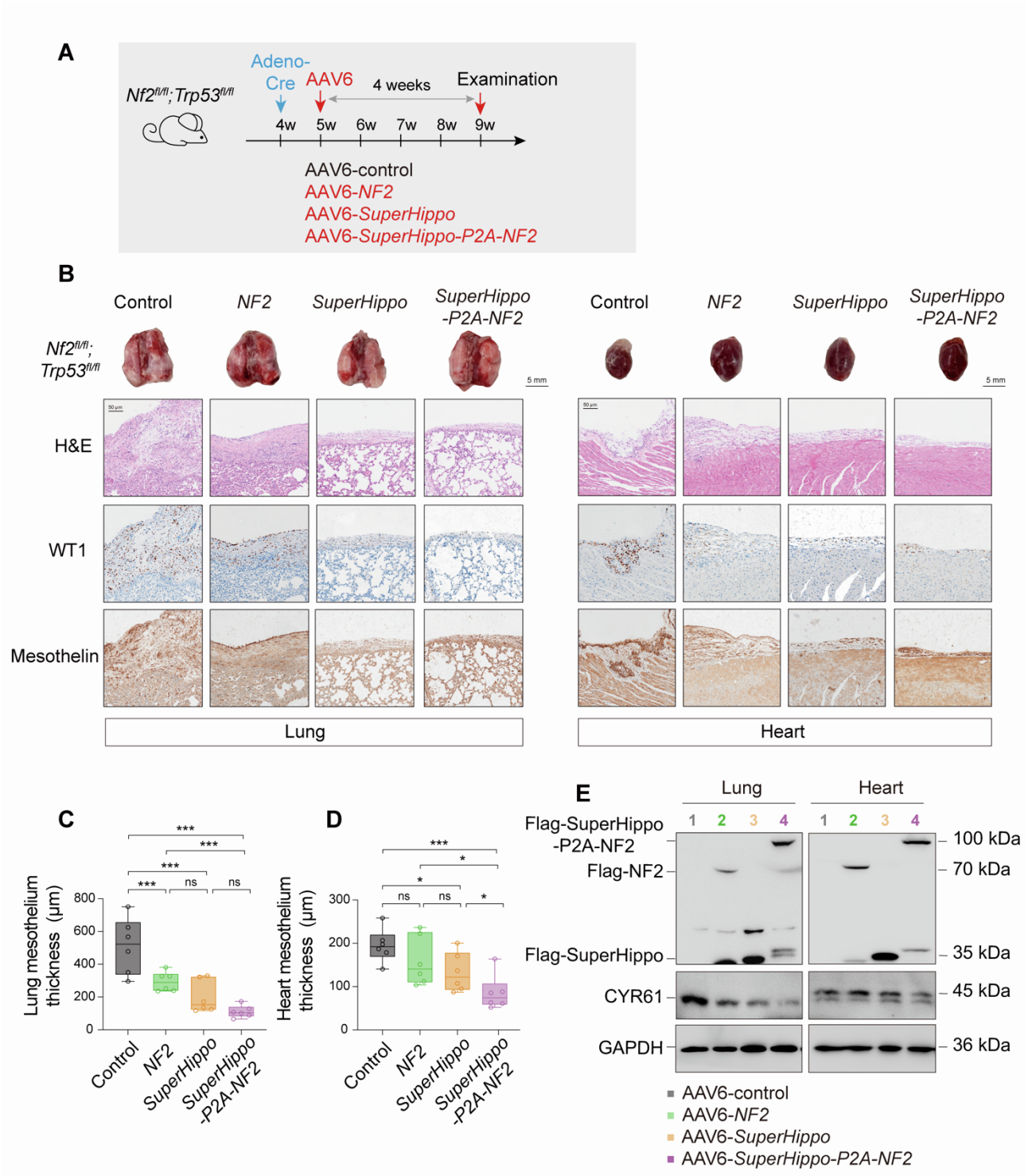

Figure S7. The efficacy of *NF2*, *SuperHippo*, or *SuperHippo-P2A-NF2* in mouse DPM model. Related to Figure 7.

(A) Schematic diagram illustrating the experimental procedure. Adeno-Cre was injected intrathoracically into 4-week-old *Nf2*$^{fl/fl}$;*Trp53*$^{fl/fl}$ mice to initiate DPM. One week later, AAV6-control, AAV6-*NF2*, AAV6-*SuperHippo*, and AAV6-*SuperHippo-P2A-NF2* were injected intrathoracically into the mice, respectively. Lungs and hearts were collected for histological analysis after an additional 4 weeks. n = 3-4 for each group.

(B) H&E and IHC staining of lung and heart tissue sections from control and treated mice. IHC for WT1 and Mesothelin was shown. Scale bar, 5 mm for gross lung and heart images, and 50 μm for H&E or IHC images.

(C and D) Measurement of the average thickness of lung and heart mesothelium in mice from control and treated groups. Mesothelium thickness is primarily defined by Mesothelin staining signals.
(E) Immunoblotting analysis of *NF2*, *SuperHippo,* and *SuperHippo-P2A-NF2* expression and cleavage in lungs and hearts from mice treated with AAV6-*NF2,* AAV6-*SuperHippo,* and AAV6-*SuperHippo-P2A-NF2*. The expression of CYR61 was also reduced in treated samples.
Data are presented as mean ± SEM. Statistical significance: *, $p < 0.05$, **, $p < 0.01$, ***, $p < 0.001$. The Student's *t*-test was used.